# Simulation of Biological Cell Sorting Using a Two-Dimensional Extended Potts Model

François Graner and James A. Glazier[a]

*Research Institute for Electrical Communications, Tohoku University, 2-1-1 Katahira, Sendai 980, Japan*

(Received 16 March 1992)

We simulate the sorting of a mixture of two types of biological cells using a modified version of the large-$Q$ Potts model with differential adhesivity. We find long-distance cell movement leading to sorting with a logarithmic increase in the length scale of homogeneous clusters. Sorted clusters then round. We find two successive phases: a rapid boundary-driven creation of a low-cohesivity cell monolayer around the aggregate, and a slower boundary-independent internal rearrangement.

PACS numbers: 87.10.+e, 64.60.Cn, 64.75.+g, 75.10.Hk

Embryonic cells of two different types, when dissociated, randomly mixed, and reaggregated, can spontaneously sort to reestablish coherent homogeneous tissues [1]. Both complete and partial cell sorting (in which large clusters of one cell type are trapped inside a continuous structure of the other type) have been observed experimentally *in vitro* in embryonic cells in two [2] as well as in three dimensions [3,4]. Sorting is a key step in the regeneration of a normal animal from aggregates of dissociated cells of adult hydra and involves neither cell division nor differentiation but only spatial rearrangement of cell positions [5,6].

Experiments have demonstrated that differences in intercellular adhesivity determine the final state of cell sorting, the cell configuration approaching the global minimum of overall surface energy [7,8]. Driving forces can arise from differential surface energies, i.e., the differences of surface energy for boundaries between like cell types (homotypic), unlike cell types (heterotypic), and cells and the external medium (edge).

Previous simulations of cell sorting on a lattice either took cells to be pointlike or used nonrealistic rules to describe topological changes [9,10]. However, cells have a nontrivial topology which must be simulated correctly if we wish to understand cell sorting. In this respect, boundary and vertex dynamic models are preferable [9]. The large-$Q$ Potts model has proved useful in simulations of diffusive grain growth driven by surface energy, and can correctly simulate experimentally observed topological changes in cellular patterns in metals and soap froths. It therefore seems a good starting point for a cell-sorting model. However, cell sorting occurs through the movement of cells rather than through cell growth. In addition, the Potts model simulates a pure material with a single surface energy, while cell sorting requires the presence of at least two different cell types. We therefore simulate cell sorting in two-dimensional aggregates using an extension of the two-dimensional Potts model which constrains cell size and allows for different surface energies between different cell types [11–15].

*Model.*—The large-$Q$ Potts model describes a collection of $N$ cells by defining $N$ degenerate spins, $\sigma(i,j) = 1,2,\ldots,N$, where $i,j$ identifies a lattice site. A cell $\sigma$ consists of all sites in the lattice with spin $\sigma$. Cells need not be simply connected. Mismatched bonds between different cells have energy 1 and bonds between like spins have energy 0. The Hamiltonian is

$$\mathcal{H}_{\text{Potts}} = \sum_{(i,j),(i',j') \text{ neighbors}} 1 - \delta_{\sigma(i,j),\sigma(i',j')}, \tag{1}$$

where the neighbors may be of any desired range on either a square or hexagonal lattice. At each step we select a lattice site at random and change its spin from $\sigma$ to $\sigma'$ with Monte Carlo probability, for a temperature $T > 0$, $P(\sigma(i,j) \rightarrow \sigma'(i,j)) = \{\exp(-\Delta\mathcal{H}/kT)$: $\Delta\mathcal{H} > 0$; 1: $\Delta\mathcal{H} \leq 0\}$, and for $T = 0$, $P(\sigma(i,j) \rightarrow \sigma'(i,j)) = \{0$: $\Delta\mathcal{H} > 0$; 0.5: $\Delta\mathcal{H} = 0$; 1: $\Delta\mathcal{H} < 0\}$, where $\Delta\mathcal{H}$ is the energy gain produced by the change. There is a critical temperature $T_c$ above which each cell dissociates. Below $T_c$, the spins coalesce into compact cells, though for finite temperatures isolated mismatched spins are possible. At $T = 0$ the cells grow by relaxation, as the pattern minimizes its total surface area. The pattern's length scale increases as cells disappear. The dynamics and statistics agree well with experiments on surface-energy-driven grain growth, e.g., in soap froth [14,16].

Cell sorting presents a slightly different problem. While the surface-energy-driving mechanism is the same as for grain growth, biological cells have generally a fixed range of sizes. Thus the pattern cannot lose energy by coarsening, since cells cannot disappear (the same constrained evolution occurs in bubbles in magnetic films) [17]. Instead, differences in contact energies between cells of different types (differential adhesion) cause cell motion which reduces the pattern's energy. To include these ideas we add an elastic-area constraint to our Hamiltonian, and introduce a second "quantum number," $\tau$, the cell *type*. In our simulations there are three cell types, "light," "dark," and "medium," $\tau \in \{l,d,M\}$. The surface energy between two cells then depends on the types of the cells. Each cell still has a unique spin, $\sigma \in \{1,\ldots,N\}$, and consists of all lattice sites with that spin, but there may be many cells of each type, i.e., with the same $\tau$. There is no simple way to introduce differential surface energies without this cell type.

We therefore write the following modified Potts-model

 

Hamiltonian:

$$\mathcal{H}_{\text{sort}} = \sum_{(i,j),(i',j') \text{ neighbors}} J\left(\tau(\sigma(i,j)),\tau(\sigma(i',j'))\right)\left(1-\delta_{\sigma(i,j),\sigma(i',j')}\right) + \lambda \sum_{\text{spin types } \sigma} [a(\sigma) - A_{\tau(\sigma)}]^2 \theta(A_{\tau(\sigma)}) , \quad (2)$$

where $\tau(\sigma)$ is the type associated with the cell $\sigma$ and $J(\tau,\tau')$ is the surface energy between spins of type $\tau$ and $\tau'$. $\lambda$ is a Lagrange multiplier specifying the strength of the area constraint, $a(\sigma)$ the area of a cell $\sigma$, and $A_\tau$ the target area for cells of type $\tau$. Because of the surface energy, each cell usually contains slightly fewer than $A_\tau$ lattice sites. Biological aggregates are usually surrounded by a fluid medium ($\tau = M$), e.g., culture solution, substrate, or extracellular matrix, which we define as a single cell with associated type, interaction energies, and unconstrained volume. We set the target area $A_M$ of the medium to be negative and include $\theta(x) = \{0: x < 0; 1: x > 0\}$, to suppress the area constraint.

We use Potts-model dynamics, with one Monte Carlo time step (MCS) defined to be 16 times the number of spins in the array; but we suppress the nucleation of heterogeneous spins by requiring that a lattice site flip only to a spin belonging to one of its neighbors. This constraint is biologically realistic for compact aggregates, though we could relax it, e.g., to allow the nucleation of medium-filled vacancies [18]. We have checked that for our initial conditions, relaxing this constraint makes no difference at $T=0$, and only a negligible difference for $T > 0$, since heterogeneous spins are energetically forbidden in the first case and very short lived in the second [18]. This dynamics allows cells to move slowly, by gradually adjusting their boundary positions, rather than jumping abruptly as in some earlier models [9,10].

Our goal is to determine whether a model of this type exhibits biologically reasonable cell sorting. In coarsening, patterns are usually characterized by their side and area distributions and their moments, as well as the exponent describing the average rate of area growth. In cell sorting, the areas are approximately fixed so the area information is not useful. The second moment of the side distribution, $\mu_2$, is a useful measure of pattern equilibration as are the homotypic, heterotypic, and edge contact lengths. We have not yet performed statistical studies of percolation thresholds and cluster sizes.

In this Letter we refer to and represent the higher-surface-energy (low-adhesivity) cells as light ($\tau = l$) and the low-surface-energy (high-adhesivity cells) as dark ($\tau = d$).

*Anisotropy, temperature, and the area constraint.*—A difference between the model and the real system is the lattice anisotropy. A unit length of boundary has a different energy depending on its orientation, creating local energy minima which tend to pin boundaries. Working with cells much larger than the lattice constant does not solve this problem because topological changes always occur on the length scale of one lattice constant. In coarsening, pinning only occurs for the nearest-neighbor square lattice, though the scaling state distributions of different lattice types can be different from the isotropic limit [16]. We therefore employ a next-nearest-neighbor square lattice which has a low anisotropy.

However, because of the area constraint, cell sorting is still sensitive to the lattice discretization. As a result, the strength of the area constraint influences the evolution. If $\lambda$ is very small or zero, the final state depends on whether there is a free surface. If there is, all the cells shrink (for positive surface energies), the light cells shrinking and disappearing faster. If there is not, dark cells replace light cells and coarsen as in the Potts model. If $\lambda$ is too large compared to $T$ and the differences between $J$'s, the pattern freezes with all cells exactly at their target area, since the energy cost of changing the cell area to flip a single spin is large compared to any possible energy gain due to boundary length reduction. For an intermediate range of $\lambda$, the initial cells rapidly grow or shrink to reach their target areas. After this transient, cells have stable areas but the pattern does not freeze, since the finite temperature allows virtual two-spin processes which conserve energy. We choose $T=10$ and this effectively fixes $\lambda$ of order 1. In this regime, $\lambda$ does not explicitly affect the relaxation of cells' shapes and positions. But the competition between the finite area constraint and surface energies causes light cells to have a slightly smaller average area than dark cells. We employ $\lambda = 1$ in the simulations discussed in this Letter.

For $T > 0$, boundaries, especially for dark cells, can crumple [17]. Cells can also interpenetrate by nucleating spins within the bulk of their neighbors so they need not be simply connected. While multiply connected cells do not seem biologically realistic, they are the inevitable result of working on a lattice at $T > 0$. However, because we simulate at low $T$, the unattached spins are few and short lived and do not appear to cause significant qualitative changes in the pattern's evolution. We can estimate the magnitude of the problem by measuring the average number of neighbors per cell. An ideal pattern of simply connected cells with threefold vertices has $\langle n \rangle = 6$; a disconnected pattern has $\langle n \rangle > 6$. We therefore perform two $T=0$ annealing steps to reduce $\langle n \rangle$ very close to 6, before calculating the statistical properties of the pattern [16,18]. This method works well in regular Potts-model simulations and we have checked that all statistical properties converge to within a few percent of their limiting values for the fully annealed pattern [16,18].

*Surface energy.*—If we rescale all of our energies $J(\tau,\tau')$ and $\lambda$ by a multiplicative constant $b$, this is equivalent to reducing the temperature by a factor of $b$. Since we consider only energy differences in our evolution dynamics the model is also insensitive to additive rescaling of the energies, provided that we also change the

spin-spin interaction energy (here set to zero) between spins within a single cell. The crucial parameters for the pattern evolution are the relative differences between the surface energies.

We assume that all energies are symmetric, i.e., $J(d,l)=J(l,d)$, and that the energy of both cell types with the medium is equal, $J(l,M)=J(M,l)=J(d,M)=J(M,d)$, leaving four parameters. We set all energies greater than 0 with cell-medium energies largest. Otherwise, the aggregate dissociates into isolated cells, a process which can occur experimentally for small changes either in the expression of cell adhesion molecules or in the medium [19].

Spontaneous cell sorting can occur if the energy between the two types is greater than the average of the two self-interactions (otherwise the cells mix to form an experimentally observed "checkerboard") [18,20] and less than the self-energy of the light cells (or the pattern will pin) [18]. The $J$'s thus obey the inequalities

$$0<J(d,d)<[J(d,d)+J(l,l)]/2<J(d,l)<J(l,l)<J(l,M)=J(d,M). \quad (3)$$

We have checked that complete cell sorting occurs over a wide range of parameters satisfying these constraints. In this Letter we take $J(d,d)=2$, $J(d,l)=11$, $J(l,l)=14$, and $J(d,M)=J(l,M)=16$.

*Results.*—We studied large-scale equilibration by examining the rounding of a square homotypic aggregate of rectangular cells of various sizes ($A=40$). After 400 MCS the initial symmetries have totally disappeared and the aggregate has become round. However, cell boundaries lie in energetically preferred directions ($k\pi/4$) as a result of the lattice anisotropy. The perimeter lengths and $\mu_2$ are stable by 400 MCS, showing that the pattern has equilibrated.

We use this equilibrated rounded aggregate [Fig. 1(a)], with random assignment of cell types, as the initial condition for the cell-sorting simulation. The initial sorting into small clusters happens very rapidly over the first few time steps, driven by the large energy difference $J(d,l)-J(d,d)=9$ acting on isolated dark cells. These clusters then merge on a longer time scale, due to their increased mass [Figs. 1(b) and 1(c) and Fig. 2(a)]. The trapping of light cells, called "partial cell sorting" [Fig. 1(d)] is observed biologically [4,7,9].

The light cells rapidly replace the dark where the aggregate contacts the medium [Fig. 2(b)] due to the energy difference $J(d,M)-J(l,l)=14$ versus $J(l,M)-J(l,l)=2$. After 300 MCS a monolayer of light cells surrounds the dark cluster, the boundary ceases to be a driving force in the evolution [Figs. 1(d)-1(f)], and the internal rearrangement becomes boundary independent.

Bulk sorting can be seen in Fig. 2(a). The homotypic boundary rapidly (in about 4 MCS) replaces the initially dominant heterotypic boundary. Its length then increases logarithmically. The total homotypic boundary of the dark cells dominates, since the light-cell edge boundary increases at the expense of the light-cell homotypic boundary. The dark cells form a single large cluster surrounded by light cells, which rounds very slowly [Figs. 1(e) and 1(f)]. This process is driven over a one-dimensional surface by the small surface tension $\gamma_{dl}=J(d,l)-[J(d,d)+J(l,l)]/2=3$, while the cells that need to move form a two-dimensional cluster. At 4000 MCS we observe the same crossover from logarithmic cluster growth to slow rearrangement if we examine the type-type correlation function. A similar crossover between surface- and bulk-driven processes occurs in the disordering transient in soap froth [21].

*Conclusion.*—An extended large-$Q$ Potts model with

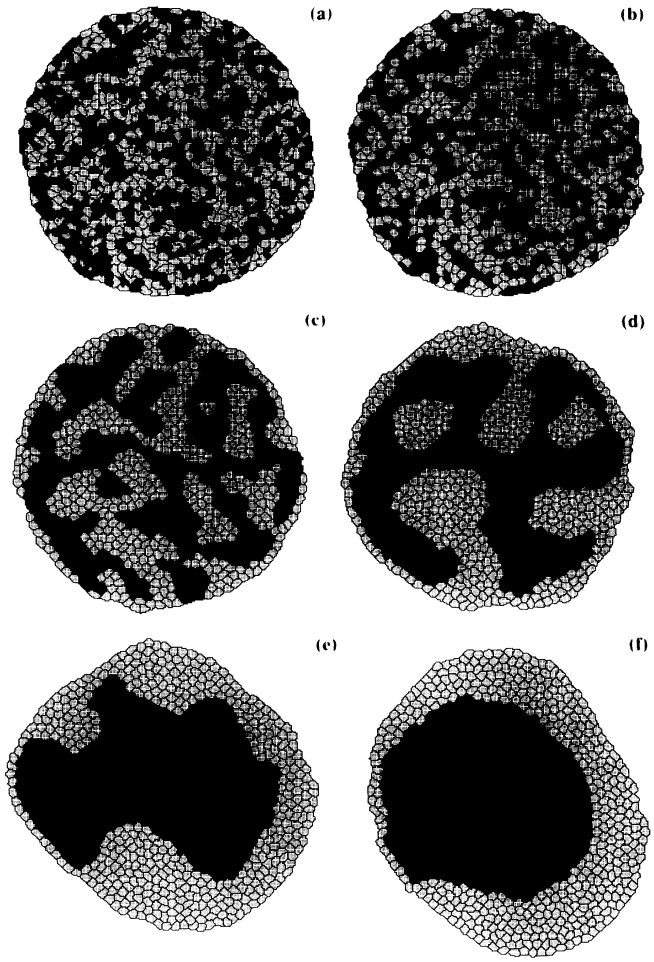


FIG. 1. Cell sorting time series. (a) Initial configuration with randomly assigned cell types, (b) 1 MCS, (c) 100 MCS, (d) 1000 MCS, (e) 4000 MCS, (f) 10000 MCS. In this figure and the following, displayed patterns and statistics are shown after two annealing steps.

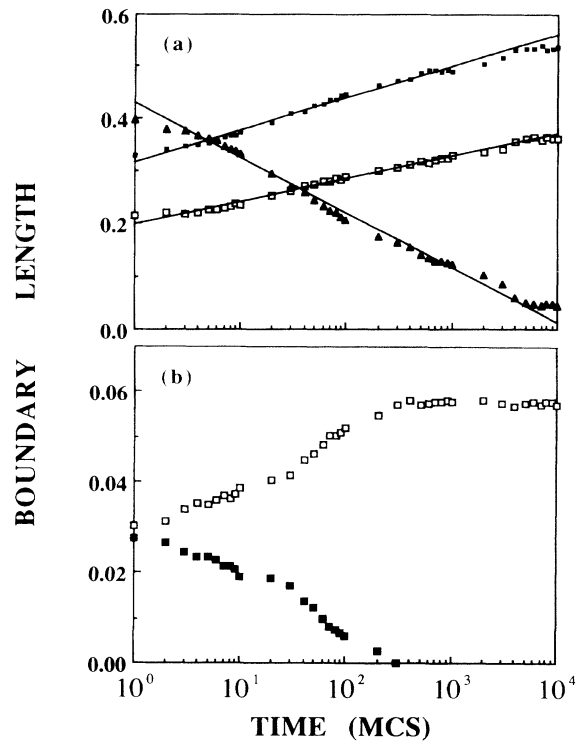


FIG. 2. Statistics on cell sorting. (a) Evolution of bulk boundary length. Lines are logarithmic fits to data between 5 and 4000 MCS, with $R^2 > 0.97$. Triangles show heterotypic boundary length; solid squares, dark-cell homotypic boundary length; and open squares, light-cell homotypic boundary length. (b) Evolution of edge boundary length. Solid squares show dark-cell edge boundary length and open squares, light-cell edge boundary length. All boundary lengths are expressed as fractions of the total boundary length.

area constraints and differential adhesivity can simulate biological cell sorting. Though the behavior of the model is robust with respect to detailed parameter choices, we are continuing to study the effects of the finite simulation temperature [18]. The model makes detailed predictions about measurable properties of biological aggregates; unfortunately, it does not appear that such experimental measurements exist. We have identified a crossover between a rapid boundary-driven stage which leads to a uniform light-cell–medium layer and partial bulk cell sorting, and a slower boundary-independent stage which leads to complete cell sorting. The latter is much slower than the former and may explain why partial cell sorting is observed biologically: The time scale for complete sorting is long compared to other biological processes.

We would like to thank Professor Yasuji Sawada for his critical reading of the manuscript and for his hospitality at Tohoku University. This research has been supported by J.S.P.S. and Monbusho.

[a]Permanent address: Department of Physics, University of Notre Dame, Notre Dame, IN 46556.

[1] J. Holtfreter, Rev. Can. Biol. **3**, 220 (1944).
[2] D. Garrod and M. Steinberg, Nature (London) **244**, 568 (1973).
[3] M. Steinberg, J. Exp. Zool. **173**, 395 (1970).
[4] P. Armstrong, Crit. Rev. Biochem. Mol. Biol. **24**, 119 (1989).
[5] K. Noda, Zool. Mag. **80**, 99 (1971) (in Japanese).
[6] A. Gierer, S. Berking, H. Bode, C. N. David, K. Flick, G. Hansmann, H. Schaller, and E. Trenkner, Nature (London), New Biol. **239**, 98 (1972).
[7] M. Steinberg, Science **141**, 401 (1963).
[8] H. Phillips and G. Davis, Am. Zool. **18**, 81 (1978).
[9] D. Sulsky, S. Childress, and J. Perkus, J. Theor. Biol. **106**, 275 (1984).
[10] M. Steinberg, J. Theor. Biol. **55**, 431 (1975).
[11] M. Anderson, D. Srolovitz, G. Grest, and P. Sahni, Acta. Metall. **32**, 783 (1984).
[12] G. Grest, D. Srolovitz, and M. Anderson, Phys. Rev. Lett. **52**, 1321 (1984).
[13] D. Srolovitz, M. Anderson, P. Sahni, and G. Grest, Acta. Metall. **32**, 793 (1984).
[14] J. A. Glazier, . Anderson, and G. Grest, Philos. Mag. B **62**, 615 (1990).
[15] J. A. Glazier, Ph.D. dissertation, University of Chicago, 1989 (unpublished).
[16] E. Holm, J. Glazier, D. Srolovitz, and G. Grest, Phys. Rev. A **43**, 2662 (1991).
[17] D. Weaire, F. Bolton, P. Molho, and J. Glazier, J. Phys. Condens. Matter **3**, 2101 (1991).
[18] J. A. Glazier and F. Graner (to be published).
[19] R-M. Mège, Médecines/Sciences **7**, 544 (1991) (in French).
[20] H. Honda, H. Yamanaka, and G. Eguchi, J. Embryol. Exp. Morph. **98**, 1 (1986).
[21] J. A. Glazier, S. P. Gross, and J. Stavans, Phys. Rev. A **36**, 306 (1987).

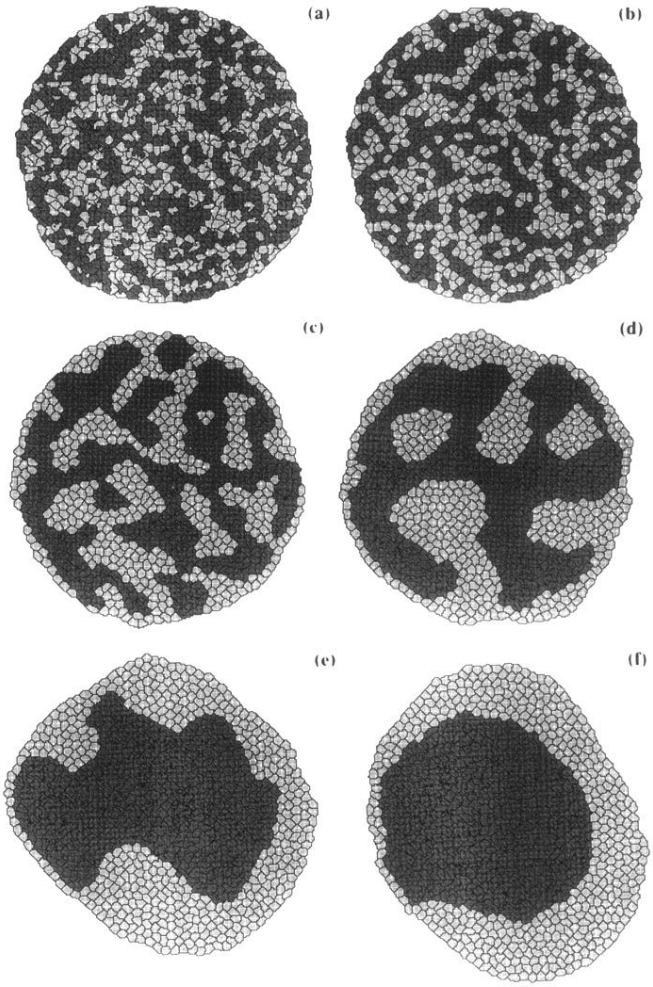


FIG. 1. Cell sorting time series. (a) Initial configuration with randomly assigned cell types, (b) 1 MCS, (c) 100 MCS, (d) 1000 MCS, (e) 4000 MCS, (f) 10000 MCS. In this figure and the following, displayed patterns and statistics are shown after two annealing steps.